Mathematical modeling of the multipair convex-concave teeth contact in precessional gearing

BOSTAN Viorel, BOSTAN Ion, and VACULENCO Maxim

The development of toothed wheels manufacturing technologies on numerically controlled machine tools (CNC) including additive technologies with 3D printing, radically changes the approaches to the presentation of curvilinear surfaces of the teeth flanks, based on mathematical models and computerized design on the CAD/CAM/CAE platform. This paradigm mainly refers to gears with non-standard profiles of multiple pair conjugated teeth with punctiform or linear contact of the active surfaces, which ensure the transformation of the motion and the transmission of the load. The paper addresses the problems of creating toothed gears $A^{D}_{CX\text{-}CV}$ for $2K{-}H$precessional transmissions, with convex-concave contact $K_{CX\text{-}CV}$ with the small difference in the curves of the flanks of the multiple pair conjugated teeth.

In order to create the convex-concave contact $K_{CX\text{-}CV}$ of the geared teeth with spherospatial motion, we admit that the profile of the satellite teeth are designated with the LEM curve of radius r.

The trajectory of the motion of the origin of the radius r in the spherospatial motion of the satellite is presented by the function $\zeta = f(\xi)$, and the profile of the teeth of the central wheels is presented by the LEM function $\zeta_1 = f(\xi_1)$.

From the Euler kinematic equations, taking into account the kinematic relation between the angles φ and ψ expressed by $\dot{\varphi} = -\frac{Z_1}{Z_2}\dot{\psi}$, we obtain the trajectory of the LEM motion $\zeta_1 = f(\xi_1)$ of origin G of the radius of the circle arcs expressed by the coordinates X_G, Y_G, Z_G depending on the rotation angle of the crankshaft ψ:

$$\begin{aligned} X_G &= R\cos\delta\,[-\cos\psi\sin(Z_1\psi/Z_2) + \sin\psi\cos(Z_1\psi/Z_2)\cos\theta] \\ &\quad - R\sin\delta\sin\psi\sin\theta, \\ Y_G &= -R\cos\delta\,[\sin\psi\sin(Z_1\psi/Z_2) + \cos\psi\cos(Z_1\psi/Z_2)\cos\theta] \\ &\quad + R\sin\delta\cos\psi\sin\theta, \\ Z_G &= -R\cos\delta\cos(Z_1\psi/Z_2)\sin\theta - R\sin\delta\cos\theta. \end{aligned} \tag{1}$$

where θ is the nutation angle, δ – angle of the conical axoid.

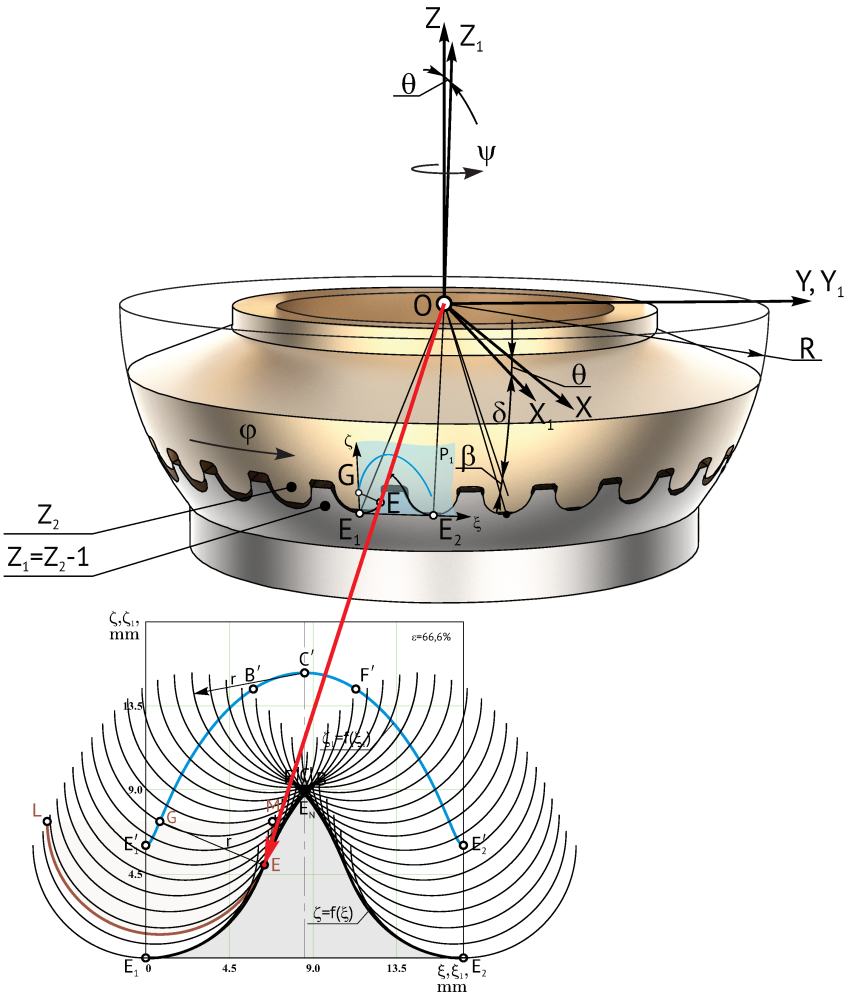

Figure 1. Description of the teeth profile of the central wheel through the wrap of the circular arcs family in the coordinate system $O\bar{X}\bar{Y}\bar{Z}$

The equation of the winding of LEM circle arc family on the sphere of radius R is determined by solving jointly the equations, which describe the surfaces of the flanks of the teeth of the satellite with a circle arc profile

$$\begin{aligned} &\Phi(X,Y,Z,\psi) = X\bar{X}_G + Y\bar{Y}_G + Z\bar{Z}_G - R\cos\beta = 0 \\ &\frac{d\Phi}{d\psi}(X,Y,Z,\psi) = 0 \end{aligned} \tag{2}$$

and the equation of the surface of the sphere

$$X^2 + Y^2 + Z^2 - R^2 = 0. \tag{3}$$

For this we write from equations (2) and (3)

$$
\begin{aligned}
\frac{d\Phi}{d\psi} &= X\frac{\partial \bar{X}_G}{\partial \psi} + Y\frac{\partial \bar{Y}_G}{\partial \psi} + Z\frac{\partial \bar{Z}_G}{\partial \psi},\\
\frac{\partial \bar{X}_G}{\partial \psi} &= \frac{\partial X_G}{\partial \psi}\cos\psi_3 - \frac{X_G}{u}\sin\psi_3 + \frac{\partial Y_G}{\partial \psi}\sin\psi_3 + \frac{Y_G}{u}\cos\psi_3,\\
\frac{\partial \bar{Y}_G}{\partial \psi} &= -\frac{\partial X_G}{\partial \psi}\sin\psi_3 - \frac{X_G}{u}\cos\psi_3 + \frac{\partial Y_G}{\partial \psi}\cos\psi_3 - \frac{Y_G}{u}\sin\psi_3,\\
\frac{\partial \bar{Z}_G}{\partial \psi} &= \frac{\partial Z_G}{\partial \psi},\\
\frac{\partial X_G}{\partial \psi} &= -R\cos\delta\,(1-\cos\theta)\cos 2\psi - R\sin\delta\sin\theta\cos\psi,\\
\frac{\partial Y_G}{\partial \psi} &= -R\cos\delta\,(1-\cos\theta)\sin 2\psi - R\sin\delta\sin\theta\cos\psi,\\
\frac{\partial Z_G}{\partial \psi} &= R\cos\delta\sin\theta\sin\psi.
\end{aligned}
\tag{4}
$$

After replacing (4) in (2) and (3) we obtain

$$
\begin{aligned}
X_O &= \frac{-(ab+de) \pm \sqrt{(ab+de)^2 + (1+a^2+d^2)(R^2b^2-e^2)}}{1+a^2+d^2}\\
Y_O &= aX_O + b, \quad Z_O = dX_O + e,
\end{aligned}
\tag{5}
$$

where,

$$
\begin{aligned}
a &= \left(\bar{X}_G\frac{\partial \bar{Z}_G}{\partial \psi} - \bar{Z}_G\frac{\partial \bar{X}_G}{\partial \psi}\right) / \left(\bar{Z}_G\frac{\partial \bar{Y}_G}{\partial \psi} - \bar{Y}_G\frac{\partial \bar{Z}_G}{\partial \psi}\right),\\
b &= \left(-R^2\cos\beta\frac{\partial \bar{Z}_G}{\partial \psi}\right) / \left(\bar{Z}_G\frac{\partial \bar{Y}_G}{\partial \psi} - \bar{Y}_G\frac{\partial \bar{Z}_G}{\partial \psi}\right),\\
d &= -\frac{\left(\bar{X}_G + a\bar{Y}_G\right)}{\bar{Z}_G}, \quad e = \frac{R^2\cos\beta - b\bar{Y}_G}{\bar{Z}_G}.
\end{aligned}
$$

Equations (5) describe the winding of the circle arc family on the sphere and represent the profile of the teeth of the central wheels. To represent the profile of the central wheel teeth in the normal section we project the winding on the sphere on a P plane and after a series of transformations we obtain the plane projection of the profile of the central wheel teeth defined by the Cartesian coordinates:

$$
\begin{aligned}
\xi &= \left\{(E_1E_2)^2 + (X-X_1)^2 + (Y-Y_1)^2 + (Z-Z_1)^2\right.\\
&\quad \left. - (X-X_2)^2 + (Y-Y_2)^2 + (Z-Z_2)^2\right\}(2E_1E_2)^{-1},\\
\zeta &= \sqrt{(X-X_1)^2 + (Y-Y_1)^2 + (Z-Z_1)^2 - \xi^2}.
\end{aligned}
\tag{6}
$$

Note: *Based on the principle of forming the winding of the circle arc family described with equations (5) with the location of their radius origins on the curve described with the function* $\zeta_1 = f(\xi_1)$ *the kinematic model of the process of generating of the central wheel teeth by spatial tumbling-rolling was developed, which reproduces the geometry and kinematics of the interaction of the teeth in the real precessional transmission.*

Position of the origins of the circular arcs G located on the curve $\zeta_1 = f(\xi_1)$ presented in (fig. 2) by p. $1, 2, 3 \ldots i$ correspond to the precession angles ψ of the crank shaft rising from one pair of teeth to the other with the angular step $\psi = 2\pi Z_2 / Z_1^2$.

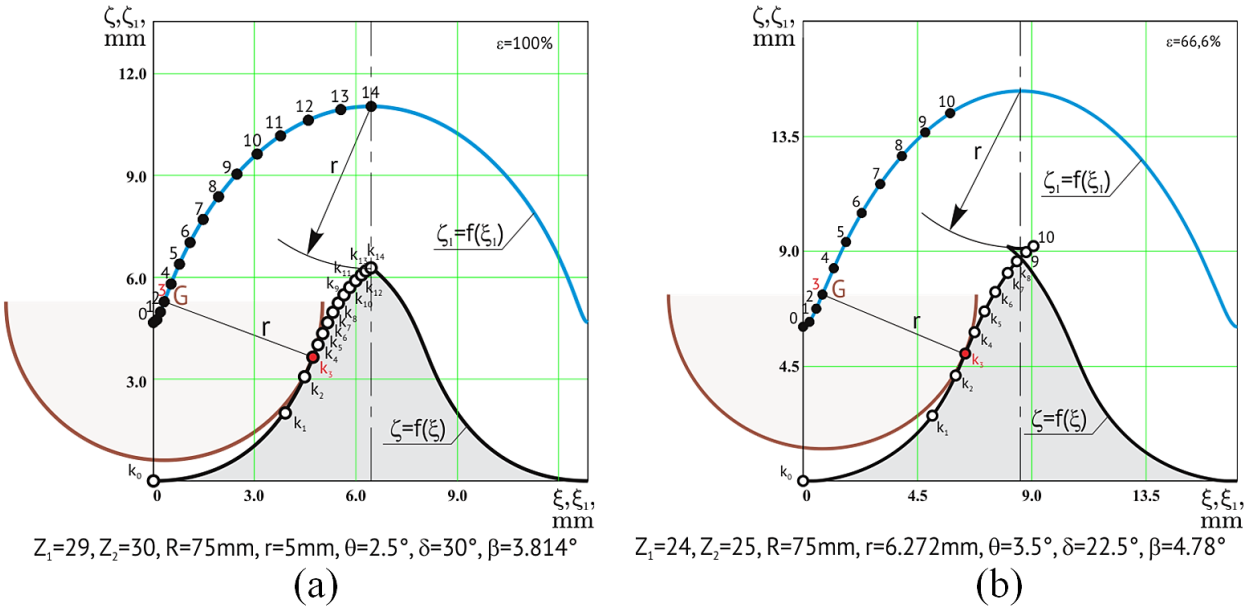

Figure 2. Active contact of the teeth in the pressional gear with frontal reference multiplicity $\varepsilon = 100\%$ (a) and $\varepsilon = 66,6\%$ (b)

Depending on the precession phase of the satellite, determined by the precession angle ψ of the crankshaft, each pair of teeth *satellite - central wheel* passes through three geometric contact forms, namely from convex-concave in the contacts k_0, k_1 and k_2, located in the foot zone of the central wheel teeth, to the convex-rectilinear in the contacts k_3 and k_4, located in the area of passage of the profile of the central wheel teeth from the concave to the convex and the convex-convex curvature in the contacts $k_5, \ldots, k_{14}$ (fig. 2 a) and $k_5, \ldots, k_8$ (fig. 2 b) respectively, located in the tip area of the central wheel teeth.

The radius of curvature at a certain point i of the teeth profile of the central wheel is calculated according to the formula

$$\rho_i = \sqrt{\left(X_i - X_{c_i}\right)^2 + \left(Y_i - Y_{c_i}\right)^2 + \left(Z_i - Z_{c_i}\right)^2} \tag{7}$$

in which X_{c_i}, Y_{c_i}, Z_{c_i} are the coordinates of the center of curvature c_i

$$X_{c_i} = \frac{\Delta 1_i}{\Delta i}, \quad Y_{c_i} = \frac{\Delta 2_i}{\Delta i}, \quad Z_{c_i} = \frac{\Delta 3_i}{\Delta i}. \tag{8}$$

where Δi, $\Delta 1i$, $\Delta 2i$ and $\Delta 3i$ are the determinants of the equation system

$$\Delta_i = \Delta X_i \left(c_i \Delta Y_{i+1} - b_i \Delta Z_{i+1}\right) + \Delta Y_i \left(a_i \Delta Z_{i+1} - c_i \Delta X_{i-1}\right) \tag{9}$$

$$+ \Delta Z_i \left(b_i \Delta X_{i+1} - a_i \Delta Y_{i+1}\right). \tag{10}$$

$$\Delta 1_i = d_i \left(\Delta Y_i \Delta Z_{i+1} - \Delta Y_{i+1} \Delta Z_i\right). \tag{11}$$

$$\Delta 2_i = d_i \left(\Delta Y_i \Delta Z_{i+1} - \Delta Y_{i+1} \Delta Z_i\right). \tag{12}$$

$$\Delta 3_i = d_i \left(\Delta Y_i \Delta Z_{i+1} - \Delta Y_{i+1} \Delta Z_i\right). \tag{13}$$

Figure 3 shows the variation of the difference of the curvature radius $(\rho k_i - r)$ of the teeth profile of the central wheel ρ_{k_i} and of the teeth of the satellite with the radius r in the contacts k_i of the conjugated flanks, depending on the precession angle ψ for the toothed gears with different parametric configuration $\left[Z_g - \theta, \pm 1\right]$.

The profiles of the teeth flanks of the central wheel are described by the function $\zeta = f(\xi)$ built according to the parametric equations of the wraping 6 of the circular arcs family of the radius r with the origin located on the trajectory of its movement $\zeta_1 = f(\xi_1)$. The profile of the satellite teeth is prescribed by a curve in circular arc with the origin of the curvature radii located on the same curve $\zeta_1 = f(\xi_1)$.

It is obvious that the bearing capacity of the gear increases if the geometry of the teeth contact has the convex-concave shape, and based on the classical theory of teeth contact as deformable bodies, the difference in radii of curvature of the conjugated flank profiles tends to be minimal.

From the perspective of decreasing energy losses in the teeth contact and researching the wear of the convex-concave contact of the teeth, we reduce the relative sliding velocity V_{al} between the teeth flanks and the distances $S_1(\psi)$ and $S_2(\psi)$ traveled by the contact points E_1 and E_2, respectively, on the profiles of the teeth of the central wheel and of the satellite according to the precession angle ψ. The distances traveled by the contact point on the profiles of the teeth of the central wheel S_1 and the satellite wheel S_2 are considered equal to the distance

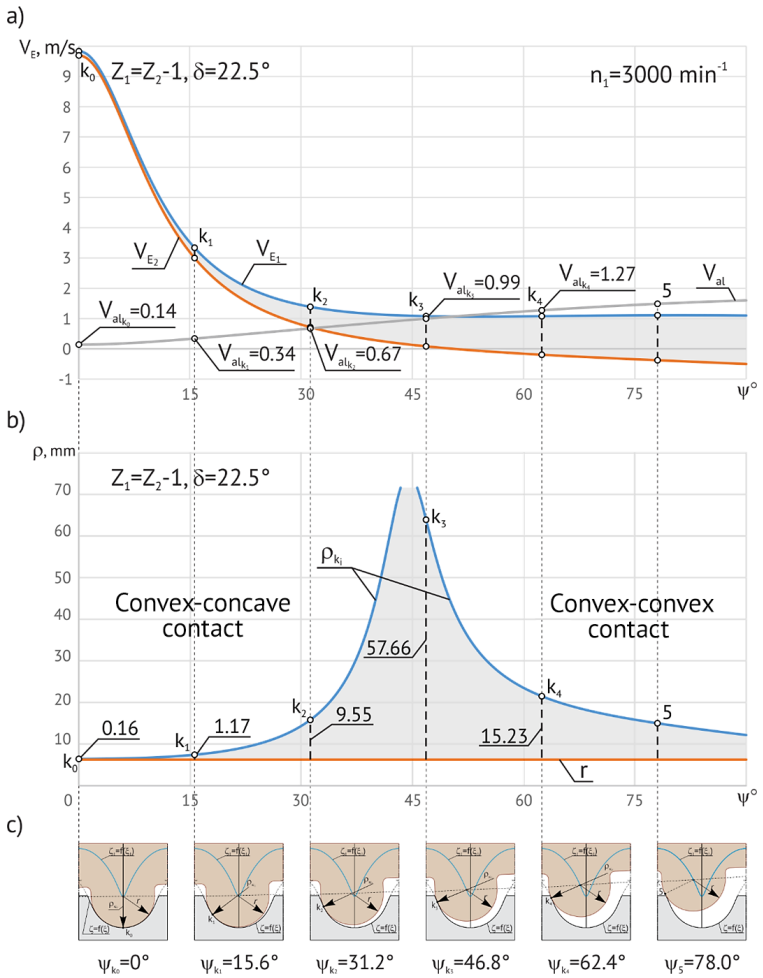

Figure 3. The linear speeds at the contact point $V_{E_1}, V_{E_2}, V_{E_3}$ (a) and the difference in curvature radii $(\rho_{k_i} - r)$ (b) of the conjugated profiles in the contact k_i (c) depending on ψ for $Z_1 = Z_2 - 1$ and $\delta = 22,5°$ ($Z_1 = 24$, $Z_2 = 25$, $\theta = 3,5°$, $\delta = 22,5°$, $r = 6,27mm$, $R = 75mm$)

traveled by them between the positions determined by the angles $\psi_{k_0} = 0$ and $\psi_{k_i} = 360 \cdot i \cdot Z_2/Z_1^2$, where $i = 1, 2, 3 \ldots$ - the order number of the contact of the pairs of conjugated teeth.

From the above, the distance traveled by the contact point E_1 on the flank of the central wheel teeth is determined by the equation:

$$S_1(\psi) = \int_0^{\frac{Z_2}{Z_1}\psi} \sqrt{\left(\frac{dx_{E_1}}{d\psi}\right)^2 + \left(\frac{dy_{E_1}}{d\psi}\right)^2 + \left(\frac{dz_{E_1}}{d\psi}\right)^2} d\psi = \int_0^t \sqrt{\dot{x}_{E_1}^2 + \dot{y}_{E_1}^2 + \dot{z}_{E_1}^2} dt, \tag{14}$$

where $\dot{x}_{E_1}$, $\dot{y}_{E_1}$ şi $\dot{z}_{E_1}$ are the projections of the velocity vector of point E_1 $\mathbf{V_{E_1}}$ on the axes X, Y and Z.

The distance traveled by the contact point in E_2 on the flank profile of the satellite wheel teeth in a circle arc for the same values of the precession angle ψ is determined by the formula:

$$\begin{aligned} S_2(\psi) &= \int_0^{\frac{Z_2}{Z_1}\psi} \sqrt{\left(\frac{dx_{1E_2}}{d\psi}\right)^2 + \left(\frac{dy_{1E_2}}{d\psi}\right)^2 + \left(\frac{dz_{1E_2}}{d\psi}\right)^2} d\psi \\ &= \int_0^t \sqrt{\dot{x}_{1E_2}^2 + \dot{y}_{1E_2}^2 + \dot{z}_{1E_2}^2} dt, \end{aligned} \tag{15}$$

where $\dot{x}_{1E_2}$, $\dot{y}_{1E_2}$ şi $\dot{z}_{1E_2}$ are the projections of the velocity vector of point E_2 on the coordinate axes x_1, y_1, z_1.

The distances $S_1(\psi)$ and $S_2(\psi)$ traveled, respectively, by the point E_1 on the flank of the central wheel tooth (14) and by the point E_2 on the flank of the satellite wheel tooth (15) in relation to time (or precession angle ψ) are defined by the integral $\int_0^t V_E dt$ and can be calculated according to Simpson's formula

$$\begin{aligned} \int_a^b f(x)dx \approx \frac{b-a}{3n} &[y_0 + (y_1 + y_3 + y_5 + \ldots + y_{n-1})\,4 \\ &+ (y_2 + y_4 + y_6 + \ldots + y_{n-2})\,2 + y_n], \end{aligned} \tag{16}$$

where, n – even number, $y_0 = f(x_0) = f(a)$; $y_i = f(x_i)$, $y_n = f(x_n) = f(b)$

For example, the distance traveled by the point E_1 on the flank of the central wheel tooth S_1 in relation to time or depending on the precession angle ψ will be:

$$\begin{aligned} S_1(t) &= \int_0^t v_{E_1} dt = \int_0^t \sqrt{\left(\dot{x}_{1E_1}\right)^2 + \left(\dot{y}_{1E_1}\right)^2 + \left(\dot{z}_{1E_1}\right)^2} dt \\ &= \int_0^\psi \sqrt{\left(\frac{dx_{E_1}}{d\psi}\right)^2 + \left(\frac{dy_{E_1}}{d\psi}\right)^2 + \left(\frac{dz_{E_1}}{d\psi}\right)^2} d\psi = \int_0^\psi \Phi(\psi)d\psi. \end{aligned} \tag{17}$$

or according to Simpson's formula $S_1(\psi)$ it takes the form

$$S_1(\psi) \approx \frac{\psi - \psi_0}{3i}\Big[\Phi_0 + \big(\Phi_1 + \Phi_3 + \Phi_5 + \ldots + \Phi_{i-1}\big)4 + \big(\Phi_2 + \Phi_4 + \Phi_6 + \ldots + \Phi_{i-2}\big)2 + \Phi_i\Big]. \tag{18}$$

Analogously, substituting V_{E_1} by V_{E_2} in the formula (17) we obtain the distance $S_2(i)$ traveled by the point E_2 on the flank of the satellite wheel tooth depending on the precession angle ψ.

The difference of the distances traveled by the points E_1 and E_2 between their common contact, for example, in k_0, corresponding to the precession angle $\psi = 0$ and their position when $\psi = \psi_i$ represents the relative sliding between the flanks of the teeth of the conjugated wheels, so

$$V_{al} = \Delta S = S_1(\psi) - S_2(\psi). \tag{19}$$

In figure 4 it is presented the variation of distances S_1 and S_2 traveled by the points E_1 and E_2 between the positions defined with the abgles ψ_{k_0} and ψ_{k_i} corresponding to the contacts $k_0 \ldots k_i$ of pairs of simultaneously engaged teeth and their difference ΔS for the toothed precessional gearing with the parameters $Z_1 = 24$, $Z_2 = 25$, $\theta = 3,5°$, $\delta = 22,5°$, $r = 6,27mm$ and $R = 75mm$.

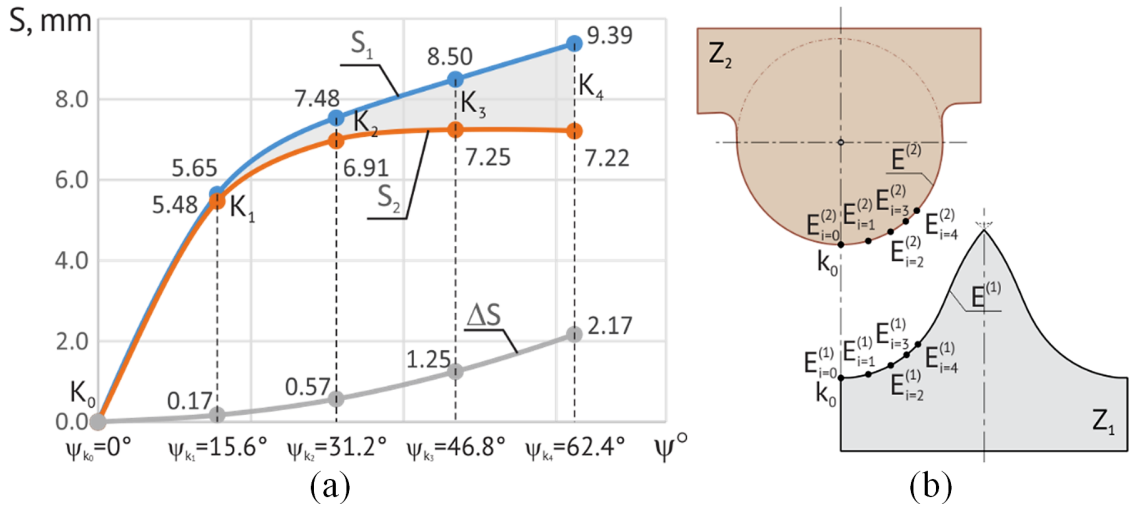

Figure 4. Distances S_1 and S_2 traveled by the contact points E_1 and E_2 between positions with ψ_{k_0} and ψ_{k_i} and their difference ΔS for the gear with the modified shape of the teeth (a) and the location topology on the profiles of the similar contact points $E_1^{(1)}$ and $E_1^{(2)}$ (b) (precessional gear $Z_1 = 24$, $Z_2 = 25$, $\theta = 3,5°$, $\delta = 22,5°$, $\beta = 4,78°$, $r = 6,27mm$, $R = 75mm$)

In figure 4 (a) there are presented the distances traveled S_1 and S_2 and their difference ΔS from the teeth contact $k_0(\psi = 0)$ and up to each teeth contacts $k_1 \dots k_4$, only for the first four pairs of bearing teeth conjugated as a result of the modification of the shape of the teeth profile of the central wheel (that transmits the load), and in figure 4 (b) it is presented the location topology on the teeth profiles of the central and satellite wheel of the contact points $E_1^{(1)}$ and $E_1^{(2)}$ for the same values of the precession angle ψ.

From the analysis in figure 4 (a) it can be observed that between the teeth contacts k_0 and k_1 corresponding to the angles $\psi = 0$ and $\psi_{k_i} \equiv \frac{2\pi i Z_2}{Z_1^2} = 15,6°$ the difference in the distances $S_1 - S_2$ made by the contact points E_1 and E_2 is only $0,17mm$, between the contacts k_0 and k_2 the difference in the distances covered is $\Delta S = 0,57mm$, between the contacts k_0 and k_3 $\Delta S = 1,25mm$, between k_0 and k_4 $-$ $\Delta S = 2,17mm$, between k_0 and k_5 $\Delta S = 3,29mm$, between k_0 and k_6 $\Delta S = 4,57mm$, between k_0 and k_7 $\Delta S = 5,94$, and between k_0 and k_8 $\Delta S = 7,35mm$.

The kinematics of the contact points k_0, k_1, $k_2 \dots k_i$ corresponding to the crank shaft positioning angles ψ_0, ψ_1, $\psi_2 \dots \psi_i$ is characterized by varying the linear speeds V_{E_1} and V_{E_2} and the relative sliding speed between the flanks $V_{al_{K_i}}$. The geometry of the teeth contact in the points k_0, k_1, $k_2 \dots k_i$ is characterized by the radii of curvature ρ_{k_i} and r of the conjugated profiles and their difference $(\rho_{k_i} - r)$. Tha analysis of the kinetics of the teeth contact is performed for the frequency of the revolutions of the crank shaft $n_1 = 3000min^{-1}$.

Thus, for the gearing corresponding to the configuration $\left[Z_g - \theta, -1\right]$ with the corration of the teeth numbers $Z_1 = Z_2 - 1$ and the angle of the conical axoid $\delta = 22,5°$ presented in figure 3 (a) the linear speed in the teeth contact k_0, $V_{E_1} = 9,83m/s$, $V_{al_{k_0}} = 0,14m/s$, and the curvature radius of the teeth profile of the central wheel $\rho_{k_0} = 6,43mm$ of the satellite wheel $r = 6,27mm$ and their difference $\rho_{k_0} - r = 0,16mm$ (see fig. 3, a).

With the increase of the angular coordinate from one conjugated pair to the other with the step $\psi = 2\pi i Z_2/Z_1^2$ for example: from the angular coordinate $\psi_{k_0} = 0°$ up to $\psi = 15,6°$ attributed to contact k_1 the linear speeds V_{E_1} and V_{E_2} decreases k_1 registering in contact k_1 the difference $V_{al_{k_1}} = V_{E_2k_1} - V_{E_1k_1} = 0.34m/s$ and the difference of the curvature radii of the conjugated flanks in k_1 $\rho_{k_1} = 1,17mm$; in contact k_2 corresponding to $\psi = 31,2°$, $V_{al_{k_2}} = 0,67m/s$ and the difference

of the curvature radii $\rho - k_2 - r = 9,55mm$; in contact k_3, corresponding to $\psi = 46,8°$ $V_{al_{k_3}} = 0,99m/s$, and the geometry of the teeth contact passes from convex-concave to convex-convex with the external curvature radius of the teeth profile of the central wheel $\rho_{k_3} = 57.66mm$. Figure 3 (c) shows the evolution of the geometry from the contact k_0 to the contact k_4.

Conclusions and recommendations

(1) The mathematical modeling of the surfaces of machine parts interpreted on computerized CAD/CAM/CAE design, research and manufacturing platforms in the near future will revolutionize the global change of machine tool park architecture of machine parts manufacturing plants and will also generate enormous social consequences in the field of training of specialists of all levels.

(2) The development of the CAD/CAM/CAE design-manufacturing platform based on mathematical models facilitates the replacement of the classic parts manufacturing processes with new manufacturing technologies on numerically controlled machine tools and additive technologies with 3D printers.

(3) The CAD/CAM/CAE platform based on mathematical models of constructive-functional interpretation of machine assemblies, changes the paradigm of achieving the idea in industrial product in much smaller terms and with much lower costs.

(4) The first three conclusions will impose harsh conditions for an essential change in the content of the training of specialists at university, college and vocational education and training professional levels.

References

[1] Бостан И. А. Прецесионные передачи с многопарным зацеплением[Transmisii precesionale cu angremaj multipar]. Штиинца, Кишинев, 1991. 356 с.

[2] Bostan, V. *Modele matematice în inginerie.* Bons Offices, Chişinău, 2014. 470 p.

[3] Bostan, I. *Transmisii Precesionale* [monogr. în 2 vol.]. Chișinău: Bons Offices, 2019. Vol. 1. 477 p., Vol. 2. 639 p. ISBN 978-9975-87-495-3.

[4] Vaculenco, M. Contribuţii la studiul preciziei de prelucrare a danturilor angrenajului precesional: Autoreferat, teză de dr. în tehnică. Cond. şt. I. Bostan. UTM. Chişinău, 2008. 32 p.

[5] Bostan, I., Dulgheru, V., Gluşco, C., Mazuru, S., Vaculenco, M. *Antologia invenţiilor. Transmisii planetare precesionale: Teoria generării angrenajelor precesionale, control dimensional, proiectare computerizată, aplicaţii industriale, descrieri de invenţie.* Vol. 2. Bons Offices, Chişinău, 2011. 542 p.

(BOSTAN Viorel, BOSTAN Ion,VACULENCO Maxim) Technical University of Moldova, Chișinău, Republic of Moldova
E-mail address: ion.bostan@cnts.utm.md